Tree Physiology 33, 891–902
doi:10.1093/treephys/tpt062

Research paper

Evaluation of the impact of frost resistances on potential altitudinal limit of trees

Guillaume Charrier[1,2,3], Hervé Cochard[1,2] and Thierry Améglio[1,2,4]

[1]INRA, UMR547 PIAF, F-63100 Clermont-Ferrand, France; [2] Clermont Université, Université Blaise Pascal, UMR547 PIAF, F-63100 Clermont-Ferrand, France; [3]Present address: Department of Botany, University of Innsbruck, Sternwartestr. 15, A-6020 Innsbruck, Austria; [4]Corresponding author UMR PIAF (INRA—Univ. Blaise Pascal), Site INRA de Crouël, 5, chemin de Beaulieu, F-63039 Clermont-Ferrand, Cedex 2, France (Thierry.Ameglio@clermont.inra.fr)

Received March 11, 2013; accepted July 19, 2013; published online September 19, 2013; handling Editor Roberto Tognetti

Winter physiology of woody plants is a key issue in temperate biomes. Here, we investigated different frost resistance mechanisms on 1-year-old branches of 11 European tree species from November until budburst: (i) frost hardiness of living cells (by electrolyte leakage method), (ii) winter embolism sensitivity (by percentage loss of conductivity: PLC) and (iii) phenological variation of budburst (by thermal time to budburst). These ecophysiological traits were analyzed according to the potential altitudinal limit, which is highly related to frost exposure. Seasonal frost hardiness and PLC changes are relatively different across species. Maximal PLC observed in winter (PLC_{Max}) was the factor most closely related to potential altitudinal limit. Moreover, PLC_{Max} was related to the mean hydraulic diameter of vessels (indicating embolism sensitivity) and to osmotic compounds (indicating ability of living cells to refill xylem conducting elements). Winter embolism formation seems to be counterbalanced by active refilling from living cells. These results enabled us to model potential altitudinal limit according to three of the physiological/anatomical parameters studied. Monitoring different frost resistance strategies brings new insights to our understanding of the altitudinal limits of trees.

Keywords: budburst, frost hardiness, living cell, tree ecophysiology, winter embolism.

Introduction

Tolerance to wintertime freezing is a key factor limiting plant survival and distribution in many ecosystems (Sakai and Larcher 1987, Pockman and Sperry 1997, Ewers et al. 2003). The ability of plants to survive freezing hinges on the resistance of living tissues and the non-living water transport system (Pratt et al. 2005). During winter, perennial plants are able to increase the tolerance of perennial parts and avoid frost exposure of sensitive parts (e.g., leaves). Freezing avoidance in buds is often considered a crucial parameter to escape late freezing events in spring (Leinonen and Hänninen 2002), when high hydration makes them especially sensitive (Rodrigo 2000).

On the one hand, plants can suffer damage (lethal in extreme cases) when intracellular water freezes or extracellular freezing of sap dehydrates cells to dangerous levels (Sakai and Larcher 1987, Améglio et al. 2001*a*). Perennial plants from temperate regions have thus developed the ability to dramatically modulate their resistance to freezing temperatures. Cold hardening starts late in the growing season as day length shortens and temperature decreases (Huner et al. 1998, Li et al. 2003). These environmental cues trigger a series of physiological and biochemical changes that induce higher resistance in the plant (Levitt 1980). Carbohydrate dynamics (especially inter-conversion of starch to soluble sugars) have been extensively investigated in terms of their relationship to frost resistance (Siminovitch et al. 1953, Sakai 1966, Morin et al. 2007, Poirier et al. 2010). Many studies also proved that water content decreases when plants harden (Chen and Li 1976, Ögren 1999, Gusta et al. 2004).

On the other hand, geographical distribution of plants is related to frost-induced embolism (Langan et al. 1997, Pockman and Sperry 1997). Winter embolism is a consequence of consecutive freeze–thaw cycles (Zimmermann 1983, Tyree and Cochard 1996, Pockman and Sperry 1997). When sap freezes, dissolved gases escape due to their very low solubility in ice (Sperry and Sullivan 1992), and these bubbles can either dissolve back into the xylem sap or expand into the xylem conduit (Yang and Tyree 1992). Mean conduit diameter is often related to winter embolism sensitivity (Davis et al. 1999, Sperry and Robson 2001, Pittermann and Sperry 2003, 2006). For coniferous species with narrow xylem conducting elements, freezing events generally cause little damage to xylem (Sperry and Sullivan 1992), but Mayr et al. (2007) observed that low water potential and numerous freeze–thaw events are critical. In ring-porous species with wide xylem conducing elements, such as *Quercus* (Cochard and Tyree 1990) or *Fraxinus* (Cochard et al. 1997), a single freeze–thaw event can embolize most xylem conduits. In diffuse-porous species (intermediate diameters), the loss of hydraulic conductivity generally increases progressively during winter, as in *Acer* (Sperry and Sullivan 1992) or *Fagus* (Borghetti et al. 1993, Cochard et al. 2001).

Different sap circulation restoring mechanisms have been characterized to date (Cochard et al. 2001, Cruiziat et al. 2002), including the development of new functional vessels and/or active refilling (Ewers et al. 2001). Several authors (Sperry et al. 1987, 1988, Hacke and Sauter 1996, Améglio et al. 2004) have investigated vessel refilling through positive pressures in xylem. Some species (i.e., *Juglans* or *Acer*) exhibit positive pressures in xylem sap during winter related to high sugar contents and osmolarity (Améglio and Cruiziat 1992, Améglio et al. 1995, 2001*b*). Positive pressures in xylem sap related to mineral nutrition and soil temperature are also observable in autumn or spring (Ewers et al. 2001), whereas in several species (mainly ring-porous and conifer species), positive pressure has never been observed.

Most studies performed on frost damages have been limited to a narrow focus: either living-cell frost resistance, hydraulic resistance to winter embolism or avoidance of spring frosts depending on timing of budburst. However, xylem embolism sensitivity, for instance, is not an exclusively physical process; as freezing-induced damages to aboveground parts may limit xylem refilling by stem-pressure mechanism (Améglio et al. 2001*b*) but not root-pressure mechanism (except in some harsh conditions; Zhu et al. 2002). Here, we monitored different types of frost resistance (vessels, living cells and timing of budburst) in several common European tree species. These species were chosen according to their differences in distribution (e.g., maximal altitudinal limit as recorded in France; Rameau et al. 1989, 1993), which we hypothesized would be closely related to frost sensitivities. We expect that these different species exposed to similar frost pressure (growing in the same local area) would present a significant enough interspecific variability in physiology to provide clues to understanding their potential altitudinal limits:

(i) hydraulic resistance is expected to be related to anatomical parameters,
(ii) living-cell resistance is expected to be related to osmotic compounds,
(iii) osmotic compounds are also expected to be involved in embolism refilling ability.

According to these relations, we expect to highlight the general mechanisms driving the altitudinal limit of trees.

Materials and methods

Plant materials

The trees were growing in two sites near Clermont-Ferrand (central France): (i) Fontfreyde (45°41′58″N, 2°59′55″E, 875 m a.s.l.) and (ii) Crouël (45°46′27″N, 3°8′36″E, altitude 338 m a.s.l.). Minimal temperatures were relatively similar between the two sample sites: with an average difference of 2.1 °C from November to April. In Fontfreyde, we sampled birch (*Betula pendula* Roth), beech (*Fagus sylvatica* L.), Scots pine (*Pinus sylvestris* L.), common oak (*Quercus robur* L.), hazelnut (*Corylus avellana* L.) and hybrid walnut (*Juglans regia* L. × *Juglans nigra* L.). In Crouël, we sampled sycamore (*Acer pseudoplatanus* L.), alder (*Alnus cordata* (Loisel.) Duby), hornbeam (*Carpinus betulus* L.), plum (*Prunus cerasifera* Ehrh.) and black locust (*Robinia pseudoacacia* L.) (Table 1). We sampled 1-year-old branches on three different trees from each species at four dates: (i) in autumn (8 November), (ii, iii) twice in mid-winter (16 January and 13 February) and (iv) at specific budburst date for each species.

Table 1. Studied tree species, altitudinal distribution, potential altitudinal limit in France (cf. Rameau et al. 1989, 1993) and sampling site: Fontfreyde (875 m a.s.l.) and Crouël (338 m a.s.l.).

Species	Altitudinal distribution	Potential altitudinal limit in France (m)	Sample site
Pinus sylvestris	1: High mountain	2000	Fonfreyde
Betula pendula	1: High mountain	2000	Fonfreyde
Acer pseudoplatanus	1: High mountain	1800	Crouël
Fagus sylvatica	1: High mountain	1700	Fonfreyde
Corylus avellana	1: High mountain	1700	Fonfreyde
Alnus cordata	2: Low mountain	1400	Crouël
Quercus robur	2: Low mountain	1300	Fonfreyde
Carpinus betulus	3: Lowland	1000	Crouël
Juglans regia	3: Lowland	800	Fonfreyde
Prunus cerasifera	3: Lowland	800	Crouël
Robinia pseudoacacia	3: Lowland	700	Crouël

Electrolyte leakage test

We performed frost hardiness tests on 1-year-old branches at every date on each tree (Zhang and Willison 1987, Sutinen et al. 1992, Charrier and Améglio 2011). We cut the samples into six 5-cm-long pieces without buds. Different pieces were cooled down to one of four sub-zero temperatures or used for two controls (unfrozen and frozen at –75 °C). In temperature-controlled boxes, cooling and warming cycles were computer-controlled by a circulator bath (Ministat Huber, Offenburg, Germany) with an external Pt100 probe in the chamber. Freezing was applied at a steady rate of –5 K h^{-1} down to –10, –20, –30 °C and either –5 °C in November and spring or –40 °C in winter. Air temperature was then held at a minimal temperature for 1 h, followed by thawing at a rate of 5 K h^{-1} back to 5 °C. Temperatures were recorded on a datalogger (Campbell, Logan, UT, USA) as 1-min averages. In addition, an unfrozen control was stored at +5 °C (control) and another control was stored in a freezer at –80 °C with freezing rate ca. –7 K h^{-1}.

After freezing treatment, we cut the samples into 5-mm-long sections and put them into glass vials with 15 ml of distilled-deionized water. The vials were shaken for 24 h at +5 °C (to limit bacterial development) on a horizontal gravity shaker (ST5, CAT, Staufen, Germany). We measured electrolytic conductivity of the solution (C_1) at room temperature with a conductimeter (Held Meter LF340, TetraCon® 325, Weilheim, Germany).

After autoclaving at +120 °C for 30 min and cooling down to room temperature, we measured conductivity again (C_2). Relative electrolytic leakage (REL) was calculated as C_1/C_2 as described in Zhang and Willison (1987). We assumed the following relationship between REL and the percentage of cellular lyses (L) for each sample:

$$\mathrm{REL} = \frac{a}{\left(1 + e^{b(c-\theta)}\right)} + d \qquad (1)$$

where θ is the test temperature, parameters a and d define asymptotes of the function and b is the slope at inflection point c. Frost hardiness level was estimated as the temperature of the inflection point (c) of the adjusted logistic sigmoid function (Eq. (1)) (Repo and Lappi 1989). Parameter estimation was performed by non-linear regression using ExcelStat ver. 7.5.2.

Hydraulic conductivity of the non-living water transport system

We immediately immersed the bottom of the 1-m-long branches under water until we measured hydraulic conductance using the Xyl'em device (Bronkhort, Montigny-les-Cormeilles, France, licenced INRA; see Cochard et al. 2000 for details). We cut 7-cm-long samples on 1-year-old segments ($n = 3$/species) immersed under water to prevent air entry into vessels. The extremities were cut again with a scalpel to form a sharp end. We first measured initial conductance (k_i) using a solution of KCl 0.1 mol l^{-1} at low pressure (0.350 kPa). After perfusion of the same solution at high pressure (140 kPa) for embolism resorption, we measured the conductance several times until maximal conductance (k_{max}) was reached. Percentage loss of conductivity (PLC) was calculated as $(k_{max} - k_i)/k_{max}$.

Water content and sap osmolarity

We extracted xylem sap from samples (40-cm-long, $n = 3$ per species) using a vacuum pump (Bollard 1953). Extracted sap was weighed (SW) (Améglio et al. 2002) and osmolarity was measured with a Roebling 13DR automatic osmometer (Messtechnik, Berlin, Germany). After xylem sap extraction, sample fresh weights (FW) were measured, before being dried for 7 days at 80 °C and weighed (DW). Water content was calculated as: (FW + SW – DW)/DW.

Extraction and quantification of soluble carbohydrates

We mixed 50 mg of lyophilized ground samples with 1 ml of mannitol solution (5 g l^{-1}) in 80% ethanol, shaken for 30 min at 80 °C, then centrifuged (10 min, 15,775 *g*, 20 °C, SR2000, Prolabo, Fontenay-sous-bois, France). We filtered the supernatant in a cartridge containing AGX-1 anion-exchange resin (150 µl), polyvinyl-polypyrrolidone (100 µl) and activated charcoal (200 µl). We mixed the solid three times with 80% ethanol (1 ml), 50% ethanol (0.5 ml) and 80% ethanol (0.5 ml) before rinsing the cartridge with 80% ethanol (1 ml). We dried liquid fraction for carbohydrate analysis and solid fraction for starch analysis.

For carbohydrate analysis, we dissolved each sample in 0.5 ml water and separated them on an Aminex-HPX87C column coupled with a refractometer (R12000, Sopares, Gentilly, France). To measure starch content, we mixed the solids with NaOH 0.02 N and autoclaved them (2 h, 120 °C, 1 bar). We incubated the samples with amyloglucosidase (1.5 h, 52 °C) in a 96-well microplate, with 12 µl ATP (5×10^{-4} mol l^{-1}), 12 µl NADP (1.4×10^{-4} mol l^{-1}), 60 µl triethanolamine buffer (triethanolamine 0.48 mol l^{-1}, magnesium sulfate 1×10^{-2} mol l^{-1}, pH = 7.6), 96 µl water and 12 µl of sample supernatant in each well. We measured the absorbance at 340 nm (Power Wave 200, BioTek Instruments, Thiais, France) as a blank and after incubation with 10 µl of hexokinase/glucose-6-phosphate dehydrogenase (EC1.1.1.49) for 40 min under shaking.

Mean vessel diameter

We sliced the samples in 20-µm-thick cross-sections on a cryomicrotome (Reichert-Jung, 2030, Vienna, Austria) with a platinum-cooled Peltier and sandwiched under glass coverslips. We sliced two cross-sections per individual on different branches ($n = 6$ per species). We took digital photos of the vessels (magnification: ×400) and processed them using the ImageJ software (http://rsb.info.nih.gov/ij). We calibrated between the samples using micrometer photos at the same magnification. We calculated the mean hydraulic diameter (D_h) from individual vessel diameter (D) as: $\Sigma D^5/\Sigma D^4$. The hydraulic diameter is relevant for hydraulic conductance within a branch (Davis et al. 1999).

Phenological and climate data

We checked, every 2 days, on five branches per tree species buds phenological stages. Date when 50% of the buds that would eventually break had reached stage 10 on the BBCH scale was calculated as the day of budburst (Meier 2001). We monitored daily maximum and minimum air temperature for each sample site by governmental weather stations (Meteo France): Saint-Genes-Champanelle: 45°43′7.58″N, 3°1′0.57″E and Aulnat: 45°47′12.67″N, 3°8′57.30″E. We calculated thermal time from 1 January until day of budburst in degree-days (DD; Arnold 1959) as: $\Sigma(T_{\mathrm{mean}} - 5)$ (if $T_{\mathrm{mean}} > 5$ °C).

Statistical analyses and modeling

We calculated linear regression and *P* values using R software (R Development Core Team 2005). We performed analysis of variance (ANOVA) and subsequent post hoc Fisher's test (least-significant difference (LSD)) to determine significant differences between groups with $\alpha = 0.05$. For correlation tests, we used Spearman's non-parametric test with $\alpha = 0.05$ after testing for normality of distribution with a Shapiro–Wilk test.

We modeled potential altitudinal limit by multiple linear regression fitted by R^2 minimization using the lm function in the R software. Selection of the best model was based on significance of parameters with higher adjusted R^2 and lower Bayesian information criterion (BIC), which qualitatively compare models according to maximum likelihood and parsimony.

Results

Frost resistance of living cells

Frost hardiness for all of the species increased from November until deep winter (frost hardening period) then decreased until budburst (dehardening) in all groups: high-mountain (Figure 1a), low-mountain (Figure 1b) and lowland species (Figure 1c). In mid-winter, mean maximal frost hardiness ($\mathrm{FH_{Max}}$) was –24.4 ± 1.0 °C in the lowland species group, which was similar to the low-mountain species group (–25.4 ± 1.1 °C) and lower than the high-mountain species group (–31.7 ± 1.3 °C). In this group, *P. sylvestris* presented a very strong $\mathrm{FH_{Max}}$ in winter (–39.7 ± 0.7 °C), but the difference was still significant (Fisher's LSD test; $P = 0.032$) without this species.

During winter, changes in frost hardiness were negatively correlated with starch content dynamics for all of the species except *A. cordata*, *A. pseudoplatanus*, *C. betulus* and *P. cerasifera* (Table 2). Soluble carbohydrate content increased with increasing frost hardiness except in *B. pendula*, *C. avellana* and *P. sylvestris*. Water content was only significantly correlated to frost hardiness

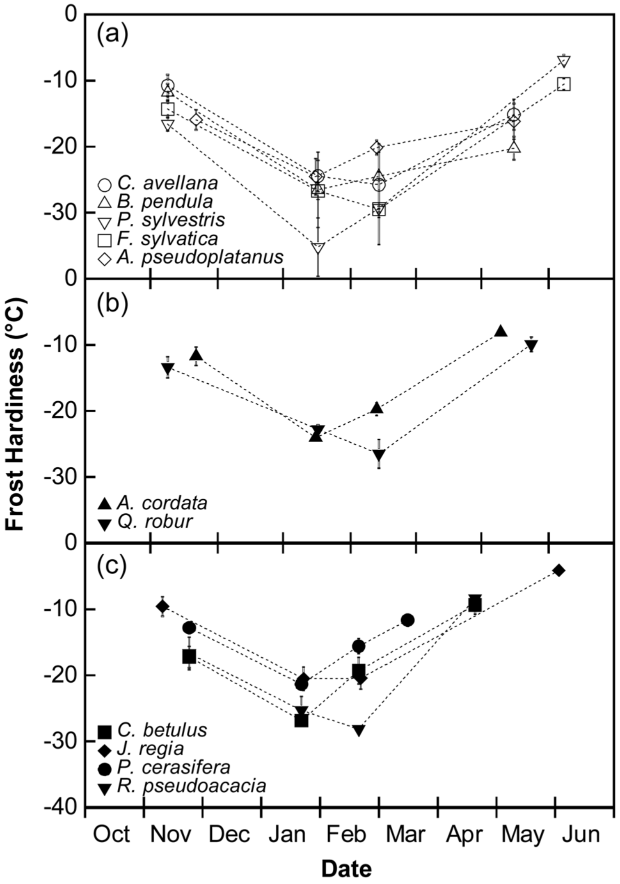

Figure 1. Seasonal change in frost hardiness (°C) of tree species according to their altitudinal distribution: high-mountain and submountain species (a), low-mountain species (b) and lowland species (c). Symbols and bars represent mean and standard errors of three replicates.

Table 2. Correlation between changes in frost hardiness and in starch content (mg $\mathrm{g^{-1}}$ DW), soluble carbohydrates content (mg $\mathrm{g^{-1}}$ DW) or water content (g $\mathrm{g^{-1}}$ DW) in different species. Numbers represent Spearman's correlation coefficient and symbols significance of correlation: $P > 0.05$; $^*P < 0.05$; $^{**}P < 0.01$; $^{***}P < 0.001$. Numbers 1–3 refer to altitudinal distribution as in Table 1. Numbers in italics indicate that the correlation is not significant.

	Species	Starch content	Soluble carbohydrates content	Water content
1	*P. sylvestris*	0.698*	*0.173*	0.651*
	B. pendula	0.618*	*−0.484*	*−0.188*
	A. pseudoplatanus	*−0.067*	−0.648*	*0.181*
	F. sylvatica	0.634*	−0.855***	*0.423*
	C. avellana	0.626*	*−0.553*	*−0.081*
2	*A. cordata*	*−0.269*	−0.797**	*0.333*
	Q. robur	0.590*	−0.807**	*0.251*
3	*C. betulus*	*0.292*	−0.867***	0.647*
	J. regia × nigra	0.746**	−0.907***	0.578*
	P. cerasifera	*0.148*	−0.801**	*0.305*
	R. pseudoacacia	0.643*	−0.583**	*0.124*

in *C. betulus*, *J. regia* × *nigra* and *P. sylvestris*. Finally, across species, $\mathrm{FH}_{\mathrm{Max}}$ was highly correlated with total non-structural carbohydrate content in November ($\mathrm{NSC}_{\mathrm{Nov}}$: starch + soluble carbohydrates, $r = -0.48$; $P = 0.005$).

Frost resistance to embolism

In the high-mountain species group, PLC remained null through winter for *C. avellana*, *B. pendula* and *P. sylvestris*, and maximal PLC ($\mathrm{PLC}_{\mathrm{Max}}$) was 43% for *A. pseudoplatanus* and 39% for *F. sylvatica* (Figure 2a). In the low-mountain species group, $\mathrm{PLC}_{\mathrm{Max}}$ was higher than 60% (Figure 2b). Seasonal changes also contrasted across species. In *Q. robur*, PLC was 100% after the first freeze–thaw cycle, while for *A. cordata*, PLC increased in winter and decreased just before budburst. In lowland species (Figure 2c), $\mathrm{PLC}_{\mathrm{Max}}$ was higher than 60% for the four species with either 100% embolism after the first freeze–thaw cycle or increase in PLC during winter followed by a decrease before budburst.

We observed three different patterns of hydraulic frost resistance: (i) complete resistance (*B. pendula, C. avellana and P. sylvestris*), (ii) complete sensitivity (*Q. robur* and *R. pseudoacacia*) and (iii) an increase of embolism during winter followed by a decrease before budburst (*A. cordata*, *A. pseudoplatanus*, *C. betulus*, *F. sylvatica* and *J. regia* × *nigra*). Furthermore, PLC generated by one freeze–thaw cycle in November ($\mathrm{PLC}_{\mathrm{AFC}}$) is related to mean hydraulic diameters of xylem conducing elements with a threshold in sensitivity around 30 µm (Figure 3).

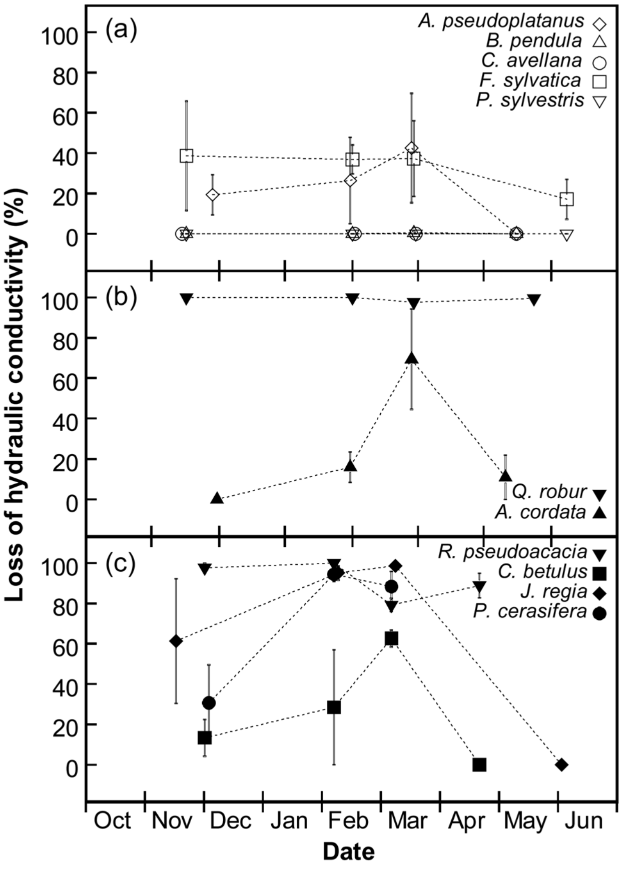

Figure 2. Seasonal change in PLC of tree species according to their altitudinal distribution: high-mountain and sub-mountain species (a), low-mountain species (b) and lowland species (c). Symbols and bars represent mean and standard error of three replicates.

Among species exhibiting total or partial embolism repair, only *F. sylvatica* and *J. regia* × *nigra* significantly increased sap osmolarity during the winter compared with autumn or spring (Figure 4a). At budburst, *B. pendula*, *C. betulus*, *C. avellana* and *P. cerasifera* also significantly increased osmolarity. Osmolarity was highly correlated to osmotic pressure generated by soluble carbohydrate ($r = 0.89$; $P < 0.001$; Figure 4b), explaining 76% of the variance in osmotic pressure.

Relation with potential altitudinal limit

Frost avoidance to late frost, evaluated based on thermal time to budburst (TT) in DD from 1 January until budburst, was early for *B. pendula*, *C. avellana*, *P. cerasifera* and *Q. robur* (150 < TT < 250DD), but late for *P. sylvestris*, *F. sylvatica*, *C. betulus*, *R. pseudoacacia*, *A. cordata* and *A. pseudoplatanus* (250 < TT < 350DD) and even later for *J. regia* × *nigra* (TT > 350DD). However, we found no significant correlation in either potential altitudinal limit ($r = -0.28$; $P = 0.12$), $\mathrm{PLC}_{\mathrm{Max}}$ ($r = 0.34$; $P = 0.054$), $\mathrm{FH}_{\mathrm{Max}}$ ($r = 0.33$; $P = 0.064$) or $\mathrm{PLC}_{\mathrm{AFC}}$ ($r = 0.30$; $P = 0.089$) (Table 4).

Significant correlations between parameters (see Table 4) were used to model potential altitudinal limits depending on the ecophysiological parameters ($\mathrm{PLC}_{\mathrm{Max}}$, $\mathrm{PLC}_{\mathrm{AFC}}$, $\mathrm{FH}_{\mathrm{Max}}$ and/or TT) or physiological parameters (D_{h}, $\mathrm{NSC}_{\mathrm{Nov}}$, $\mathrm{Starch}_{\mathrm{Min}}$, $\mathrm{Raffi}_{\mathrm{Max}}$, $\mathrm{WC}_{\mathrm{Max}}$ and/or $\mathrm{WC}_{\mathrm{Min}}$). According to the ecophysiological parameters, the most significant and parsimonious model ($R^2_{\mathrm{adj}} = 0.602$; $P < 0.001$; and BIC = 478.89) was dependent on only one parameter, $\mathrm{PLC}_{\mathrm{Max}}$ (Table 5). As $\mathrm{PLC}_{\mathrm{Max}}$ appeared strongly correlated to both $\mathrm{FH}_{\mathrm{Max}}$ and $\mathrm{PLC}_{\mathrm{AFC}}$ ($R^2 = 0.774$; $P < 0.001$) without correlation

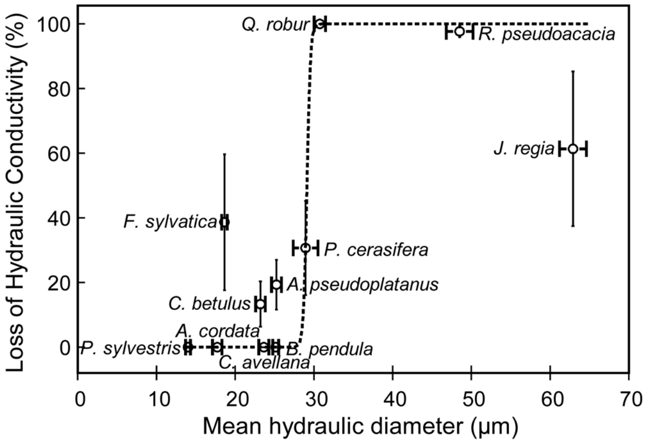

Figure 3. Relationship between PLC after one freeze-thaw cycle and mean hydraulic diameter of vessels. The dotted line plots the sigmoid fit of data.

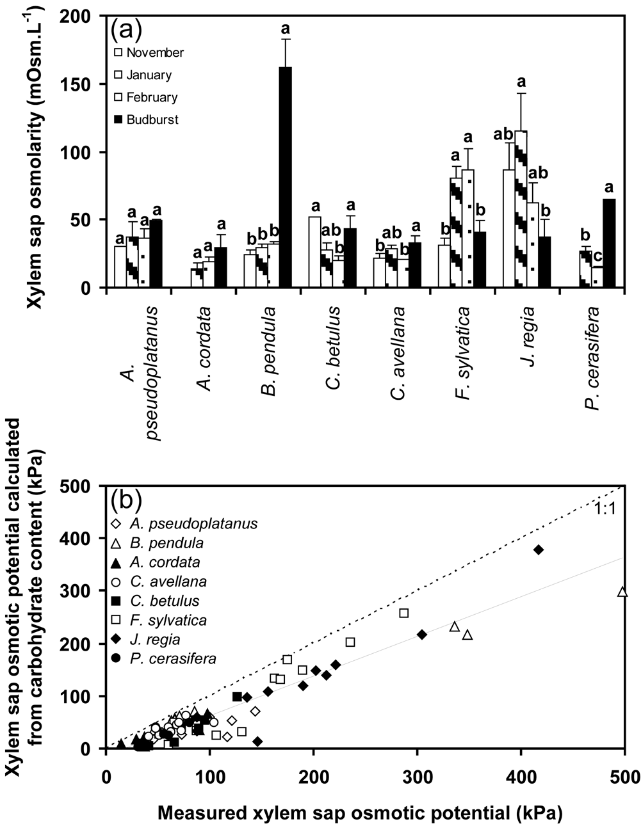

Figure 4. (a) Sap osmolarity of species measured wherever possible during winter. Letters indicate significantly different groups within a given species by ANOVA and Fisher's test (LSD) with $\alpha = 5\%$. (b) Relationship between sap osmolarity and soluble sugar concentration (glucose, fructose and sucrose: GFS) measured from xylem sap in species that increased PLC during winter then decreased PLC before budburst. The GFS is expressed in osmotic pressure units as calculated from total concentration of the three component sugars. The coefficient of determination ($R^2 = 0.871$, $P < 0.001$) of the linear regression is presented.

Table 3. Thermal time ± SE (in DD base 5 °C) calculated from 1 January until budburst for different species (if $T_{\mathrm{mean}} > 5$ °C: $\mathrm{TT} = \Sigma(T_{\mathrm{mean}} - 5)$). Numbers 1–3 refer to altitudinal distribution as in Table 1.

	Species	Thermal time for budburst (DD)
1	*P. sylvestris*	300 ± 0
	B. pendula	155 ± 0
	A. pseudoplatanus	342 ± 39
	F. sylvatica	300 ± 0
	C. avellana	155 ± 0
2	*A. cordata*	305 ± 26
	Q. robur	222 ± 1
3	*C. betulus*	304 ± 14
	J. regia × nigra	402 ± 2
	P. cerasifera	175 ± 5
	R. pseudoacacia	307 ± 12

across them ($R^2 = 0.082$; $P = 0.105$), potential altitudinal limit was also modeled based on significantly correlated physiological and/or anatomical parameters (D_h, $\mathrm{NSC_{Nov}}$, $\mathrm{Starch_{Min}}$, $\mathrm{Raffi_{Max}}$, $\mathrm{WC_{Max}}$ and $\mathrm{WC_{Min}}$; Table 4). All of the parameters were significant, and the most significant and parsimonious model was obtained with three of them: D_h, $\mathrm{NSC_{Nov}}$ and $\mathrm{WC_{Max}}$ ($P < 0.001$; $R^2_{\mathrm{adj}} = 0.726$ and BIC = 471.28; Table 5). Other parameters did not significantly improve the model. These results suggest that D_h, $\mathrm{NSC_{Nov}}$ and $\mathrm{WC_{Max}}$ could have an indirect effect on potential altitudinal limit via direct causal relationship with $\mathrm{PLC_{Max}}$, $\mathrm{PLC_{AFC}}$ or $\mathrm{FH_{Max}}$ as indicated (Figure 5a). The best model explained 73% of the variance with RMSE = 250 m (Figure 5b).

Table 4. Correlation coefficients according to Spearman's test between potential altitudinal limit or frost resistance-related parameters (maximal PLC ($\mathrm{PLC_{Max}}$), frost hardiness ($\mathrm{FH_{Max}}$) or PLC after one freeze–thaw cycle ($\mathrm{PLC_{AFC}}$)) and frost resistance-related parameters ($\mathrm{PLC_{Max}}$, $\mathrm{FH_{Max}}$, $\mathrm{PLC_{AFC}}$, and thermal time) or physiological parameters (diameter of vessels hydraulically weighted (D_h) or not (D_v), non-structural carbohydrate in November ($\mathrm{NSC_{Nov}}$), maximal soluble carbohydrate content (Soluble $\mathrm{carbohydrates_{Max}}$), maximal raffinose content ($\mathrm{Raffinose_{Max}}$), minimal starch content ($\mathrm{Starch_{Min}}$) and minimal or maximal water content ($\mathrm{WC_{Min}}$ and $\mathrm{WC_{Max}}$, respectively)). Significance of correlation is indicated by: $^*P < 0.05$; $^{**}P < 0.01$; $^{***}P < 0.001$ and the relationships used for altitudinal limit modeling are in bold (cf. text and Figure 5).

	Altitudinal limit	$\mathrm{PLC_{max}}$	$\mathrm{FH_{max}}$	$\mathrm{PLC_{AFC}}$
$\mathrm{PLC_{Max}}$	**−0.80*****		**0.60*****	**0.82*****
$\mathrm{FH_{Max}}$	**−0.64*****	**0.60*****		0.30
$\mathrm{PLC_{AFC}}$	**−0.60*****	**0.82*****	0.30	
Thermal time	−0.28	0.34	0.33	0.30
D_h	**−0.63*****	**0.67*****	**0.47****	**0.61*****
D_v	−0.44**	0.52**	0.26	0.55***
$\mathrm{NSC_{Nov}}$	**0.67*****	**−0.55*****	**−0.48****	**−0.38***
Soluble $\mathrm{carbohydrates_{Max}}$	−0.17	0.32	0.17	0.23
$\mathrm{Raffinose_{Max}}$	−0.64***	−0.56***	−0.55***	−0.42*
$\mathrm{Starch_{Min}}$	−0.73***	0.77***	0.41*	0.71***
$\mathrm{WC_{Max}}$	**0.50****	**−0.43***	**−0.28**	**−0.34**
$\mathrm{WC_{Min}}$	0.41*	−0.51**	−0.11	−0.60***

Discussion

Frost resistance of living cells

Electrolyte leakage is widely used as a method to monitor frost hardiness in different tissues (Sutinen et al. 1992, Charrier and Améglio 2011, Stattin et al. 2012). All of the species harden in autumn and deharden prior to budburst. The timing of frost hardening or dehardening development (date of beginning, end and rate) could have been useful to evaluate potential risks in autumn or spring, but would require far more sampling dates on all 11 species. Here, we focused on $\mathrm{FH_{Max}}$ (in January or February) as a good descriptor of specific maximal resistance level (Larcher and Mair 1968, Nilsson and Walfridsson 1995, Morin et al. 2007). At the intra-specific level, $\mathrm{FH_{Max}}$ has never been observed to differ significantly among environmental conditions (Larcher and Mair 1968, Bower and Aitken 2006,

Table 5. Comparison between different models of potential altitudinal limit depending on ecophysiological (PLC_{Max}, FH_{Max}, PLCAFC and TT) or physiological/anatomical parameters (D_h, NSC_{Nov}, WC_{Max}, WC_{Min}, $Raffi_{Max}$ and $Starch_{Min}$). RSE, adjusted R^2, degree of freedom, *F*-statistic, *P*-values, BIC and degrees of significance of different variables (***, <0.001; **, <0.01; *, <–0.05;>–0.05) are indicated.

Altitudinal limit depending on	Ecophysiological parameters	PLC_{Max}	FH_{Max}	PLC_{AFC}	TT			df	*F*-stat	*P* value	RSE	R^2	R^2_{adj}	BIC
		$6.93e^{-8}$***	–	–	–			31	49.33	$6.93e^{-8}$	301.6	0.614	0.602	478.89
		–	$2.02e^{-5}$***	–	–			31	25.22	$2.02e^{-5}$	360.6	0.449	0.431	490.66
		–	–	$1.65e^{-3}$**	–			31	11.88	$1.65e^{-3}$	412.8	0.277	0.254	499.60
		–	–	–	0.16			31	2.07	0.160	470.1	0.063	0.032	508.17
		$5.04e^{-4}$***	0.211	–	–			30	25.99	$2.83e^{-7}$	298.6	0.634	0.610	480.63
		–	$8.90e^{-5}$***	$6.67e^{-3}$**	–			30	19.90	$3.15e^{-6}$	323.6	0.570	0.542	485.93
		0.028*	0.183	0.607	–			29	16.99	$1.47e^{-6}$	302.3	0.637	0.600	483.82
		0.025*	0.237	0.701	0.522			28	12.59	$5.51e^{-6}$	305.4	0.643	0.592	486.83
	Physiological/ anatomical parameters	D_h	NSC_{Nov}	WC_{Max}	WC_{Min}	$Raffi_{Max}$	$Starch_{Min}$							
		$7.96e^{-6}$***	–	–	–	–	–	31	28.58	$7.96e^{-6}$	350.3	0.480	0.463	488.75
		–	$7.93e^{-6}$***	–	–	–	–	31	28.59	$7.93e^{-6}$	350.2	0.480	0.463	488.74
		–	–	$9.90e^{-4}$***	–	–	–	31	13.23	$9.90e^{-4}$	406.5	0.299	0.277	498.58
		–	–	–	$4.24e^{-3}$**	–	–	31	9.53	$4.24e^{-3}$	424.7	0.235	0.210	501.46
		–	–	–	–	$1.76e^{-4}$***	–	31	18.15	$1.76e^{-4}$	385.6	0.369	0.349	495.10
		–	–	–	–	–	$1.52e^{-5}$***	31	26.22	$1.52e^{-5}$	357.4	0.458	0.441	490.08
		$5.37e^{-5}$***	$5.35e^{-5}$***	–	–	–	–	30	35.11	$1.39e^{-8}$	270.1	0.701	0.681	474.00
		$2.36e^{-3}$**	$2.16e^{-5}$***	0.020*	–	–	–	29	29.33	$6.37e^{-9}$	250.0	0.752	0.726	471.28
		$2.51e^{-4}$***	$7.56e^{-5}$***	–	0.048*	–	–	29	27.35	$1.34e^{-8}$	256.6	0.739	0.712	472.99
		$7.82e^{-5}$***	$5.15e^{-3}$**	–	–	0.088	–	29	26.09	$2.21e^{-8}$	261.0	0.730	0.702	474.13
		$1.46e^{-4}$**	$9.72e^{-4}$***	–	–	–	0.100	29	25.84	$2.44e^{-8}$	261.9	0.728	0.700	474.36
		$2.43e^{-3}$**	$4.75e^{-5}$***	0.186	0.572	–	–	28	21.56	$3.26e^{-8}$	252.9	0.755	0.720	474.39
		$4.36e^{-3}$**	$4.47e^{-3}$**	0.087	0.770	0.043*	–	27	20.31	$2.18e^{-8}$	238.5	0.790	0.751	472.80
		0.010*	$8.88e^{-3}$**	0.106	0.863	0.065	0.610	26	16.51	$9.28e^{-8}$	241.8	0.792	0.744	475.96

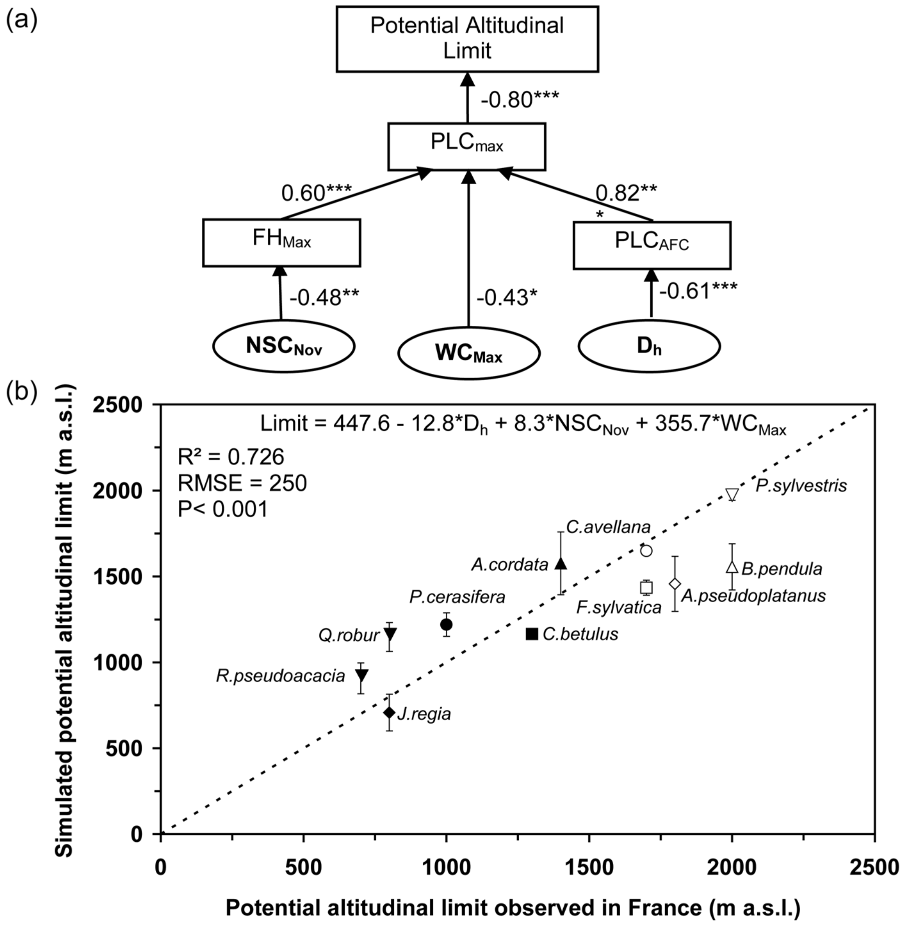

Figure 5. Schematic representation of how the most significant parameters are linked in relation to potential altitudinal limit. PLC_{Max}, maximal loss of hydraulic conductivity in winter; FH_{Max}, maximal frost hardiness; PLC_{AFC}, loss of hydraulic conductivity after one freeze–thaw cycle; NSC_{Nov}, non-structural carbohydrates in November; D_h, hydraulically weighted mean diameter of vessels; WC_{Min}, minimal water content (a). Relationship between potential altitudinal limit and value predicted by the linear model using NSC_{Nov}, D_h and WC_{min} as input variables (b).

Charrier et al. 2011). Even though small differences are observed across ecotypes, inter-specific variability is higher.

FH_{Max} was correlated to NSC_{Nov} (Table 4), as already described by Morin et al. (2007) in *Quercus*. Non-structural carbohydrate contents are the main components of plant carbon balance (Chapin et al. 1990, Le Roux et al. 2001) and indicate carbon limitation in timberline ecotones (Körner 1998, Hoch and Körner 2003, Shi et al. 2008, Bansal and Germino 2009). Non-structural carbohydrate contents play an active role in frost hardiness via starch hydrolysis into soluble sugars (Sakai 1966, Sauter et al. 1996, Améglio et al. 2004, Poirier et al. 2010) or, in *P. sylvestris*, other compounds such as amino acids, lipids or macromolecules (Lasheen and Chaplin 1971, Zwiazek et al. 2001). Frost hardiness is also related to raffinose in angiosperms (Thomas et al. 2004) and conifers (Strimbeck et al. 2008). Water content changes were only significant for a few species (e.g., *C. betulus*, *J. regia* × *nigra* and *P. sylvestris*), although the relationship has been demonstrated in many other studies (Tanino et al. 1990, Ögren 1999, Gusta et al. 2004, Charrier and Améglio 2011).

Frost resistance to embolism of non-living water transport systems

Some species are highly embolism resistant (*B. pendula*, *C. avellana* and *P. sylvestris*), whereas others are highly embolism sensitive (*Q. robur* and *R. pseudoacacia*). Freeze–thaw-induced cavitation may be considered a purely physical process due to water potential deficit (Mayr and Charra-Vaskou 2007), number of freeze–thaw cycles (Mayr et al. 2007) and diameter of xylem vessels (Davis et al. 1999, Pratt et al. 2005). Thus, PLC observed after one freeze–thaw event (PLC_{AFC}) appears strongly correlated to large mean hydraulic diameter of vessels (D_h Figure 3) and low minimal water content (WC_{Min} Table 4). Without water stress, woody plants with D_h lower than 30 μm are resistant to freeze–thaw-induced cavitation, whereas those with D_h higher than 30 μm are sensitive (Davis et al. 1999). So far, this threshold in sensitivity is mainly observed on cavitation induced in the lab (Pittermann and Sperry 2003, Pratt et al. 2005, Stuart et al. 2007, Pittermann 2010), but it has also been observed from data collected in field conditions at intra-specific (Schreiber et al. 2013) or inter-specific level (Figure 3).

In winter, some species are able to actively refill their vessels via water movements (Sakr et al. 2003). Here, we could not differentiate stem xylem pressure (Améglio et al. 2001*b*, 2004) and root xylem pressure (Ewers et al. 2001) as xylem pressure was not monitored. Root pressure is a probable mechanism of embolism repair in species that significantly decreased PLC before budburst (Figure 2: *A. pseudoplatanus*, *A. cordata*, *C. betulus*, *F. sylvatica* and *J. regia* × *nigra*). It has been identified in *A. pseudoplatanus*, *F. sylvatica* and *J. regia* × *nigra* but the results suggest it could be more widely distributed than these few observations indicate.

Sap osmotic pressure (Figure 4a) and sap-soluble carbohydrate content dynamics (Figure 4b) indicate that stem pressure could be involved in refilling in *F. sylvatica* and *J. regia* × *nigra* during winter and probably also in *B. pendula* at the budburst. Surprisingly, this relationship was not observed for *A. pseudoplatanus* despite carbohydrates being found in xylem sap during winter (Milburn and Zimmermann 1986, Tyree and Yang 1992, Cirelli et al. 2008).

Finally, correlations between $\mathrm{PLC_{AFC}}$ and $\mathrm{Starch_{Min}}$, $\mathrm{Raffi_{Max}}$ or $\mathrm{NSC_{Nov}}$ suggested that the sampling date was too late after the freeze–thaw cycle (3 days) and that some species were already refilling their vessels (as suggested in Figure 3 with *F. sylvatica* and *J. regia* × *nigra* away from the curve). $\mathrm{PLC_{max}}$ is influenced by embolism formation (due to wide xylem elements) and refilling ability, which depends on living cells. Thus, $\mathrm{PLC_{Max}}$ is directly related to vessel ($\mathrm{PLC_{AFC}}$) and living-cell ($\mathrm{FH_{Max}}$) resistances and indirectly related to physiological or anatomical parameters explaining these resistances (D_h, $\mathrm{NSC_{Nov}}$, $\mathrm{Starch_{Min}}$, $\mathrm{Raffi_{Max}}$, $\mathrm{WC_{Max}}$ and $\mathrm{WC_{Min}}$: Table 4).

Frost resistances and altitudinal limit

There was large inter-specific variability in budburst date across species (3 months from 27 February until 27 May). Thermal time to budburst is spread from 155 DD in *B. pendula* or *C. avellana* to 402 DD in *J. regia* × *nigra* (Table 3). We found no relationship with potential altitudinal limit. This is surprising, but similar correlations (between day of budburst and location) have only previously been observed in intra-specific comparisons along a latitudinal (*P. abies* in Leinonen and Hänninen 2002) or altitudinal gradient (*A. pseudoplatanus*, *F. excelsior*, *Q. petrae* and *F. sylvatica* in Vitasse et al. 2009). Even if dormancy release is controlled by chilling exposure, some species are chilling-insensitive (Morin et al. 2009). Ecodormancy could also be under photoperiod control (Caffarra and Donelly 2011), which would help avoid late freezing damages, and thus the risks limiting the impact on growing season length and carbon balance.

Carbon reserves are a crucial parameter involved in plant cell frost resistance and ability to refill embolized vessels. Vessel hydraulic integrity is the key physiological process in plant survival (Pratt et al. 2008, 2010). It is also related to altitudinal (Tyree and Cochard 1996, Langan et al. 1997, Pockman and Sperry 1997) or latitudinal distribution of species (Stuart et al. 2007). However, frost resistance to winter embolism can be addressed via two different focuses: physical resistance to embolism formation ($\mathrm{PLC_{AFC}}$) and the resistance of living cells that can actively refill vessels ($\mathrm{FH_{max}}$). Very few studies have monitored hydraulic and living-cell resistances concomitantly. Medeiros and Pockman (2010) found that freezing tolerance increases in leaves and xylem under drought conditions, but Feild and Brodribb (2001) arrived at the opposite conclusion on 12 tree and shrub species from treeline in Tasmania. Schreiber et al. (2013) found significant correlations between anatomy, frost hardiness in late summer and growth ability in a boreal planting environment in different hybrid poplar clones. Narrow vessels seem to be an important adaptive trait in frost-exposed environments.

According to our findings, hydraulic architecture integrity is not only critical for trees under drought conditions (Choat et al. 2012), but also during winter freezing conditions. Based on the correlations presented in Table 4, we modeled potential altitudinal limit depending on ecophysiological or physiological parameters (Table 5). While wood anatomy (D_h) appears to be the main driver of altitudinal limit, osmotic-related parameters ($\mathrm{GNS_{Nov}}$ and WC) are also highly significant. This relation could be generalized in different environmental conditions with genotypic effect and interactions.

Conclusions

This study brings new insights into the physiology of frost resistances at the altitudinal limit of species distributions. To survive under extreme climatic conditions, both living cells and non-living water transport systems should be resilient to freezing events. Some clear interactions were observed between two processes (embolism and refilling) that hinge on the contribution of living cells undamaged by frost to the development of pressurization mechanisms. After freezing damage, a reduction in refilling ability could lead to reduced bud survival, inducing a loss of carbon (spent to build new structures and reducing carbon assimilation period). This study highlights some important traits (i.e., NSC content, sap osmolarity or mean diameter of vessels) that should be taken into consideration in studies on frost resistance strategies in trees.

Acknowledgments

The authors thank Christian Bodet and Christophe Serre for their help with REL and PLC data collection, and Brigitte Girard, Brigitte Saint-Joanis and Marc Vandame for their input on biochemical analysis. We also thank Auvergne Traduction Technique (A.-T.-T.) for proof reading the manuscript and anonymous reviewers for their helpful comments.

Conflict of interest

None declared.

Funding

This work was supported in part by the INRA's Agronomy and Environment Department and by an MRES PhD grant for G.C.

References

Améglio T, Cruiziat P (1992) Tension pressure alternation in walnut xylem sap during winter—the role of winter temperature. C R Acad Sci Paris Sér III 315:429–435.

Améglio T, Cruiziat P, Beraud S (1995) Alternance tension/pression de la sève dans le xylème chez le noyer pendant l'hiver. Conséquences sur la conductance hydraulique des rameaux. C R Acad Sci Paris Sér III 318:351–357.

Améglio T, Cochard H, Ewers FW (2001*a*) Stem diameter variations and cold hardiness in walnut trees. J Exp Bot 52:2135–2142.

Améglio T, Ewers FW, Cochard H, Martignac M, Vandame M, Bodet C, Cruiziat P (2001*b*) Winter stem xylem pressure in walnut trees: effects of carbohydrates, cooling and freezing. Tree Physiol 21:387–394.

Améglio T, Bodet C, Lacointe A, Cochard H (2002) Winter embolism, mechanisms of xylem hydraulic conductivity recovery and springtime growth patterns in walnut and peach trees. Tree Physiol 22:1211–1220.

Améglio T, Decourteix M, Alves G, Valentin V, Sakr S, Julien JL, Petel G, Guilliot A, Lacointe A (2004) Temperature effects on xylem sap osmolarity in walnut trees: evidence for a vitalistic model of winter embolism repair. Tree Physiol 24:785–793.

Arnold CY (1959) The determination and significance of the base temperature in a linear heat unit system. Proc Am Soc Hortic Sci 74:430–445.

Bansal S, Germino MJ (2009) Temporal variation of nonstructural carbohydrates in montane conifers: similarities and differences among developmental stages, species and environmental conditions. Tree Physiol 29:559–568.

Bollard EG (1953) The use of tracheal sap in the study of apple-tree nutrition. J Exp Bot 4:363–368.

Borghetti M, Leonardi S, Raschi A, Snyderman D, Tognetti R (1993) Ecotypic variation of xylem embolism, phenological traits, growth parameters and allozyme characteristics in *Fagus sylvatica*. Funct Ecol 7:713–720.

Bower AD, Aitken SN (2006) Geographic and seasonal variation in cold hardiness of whitebark pine. Can J For Res 36:1842–1850.

Caffarra A, Donelly A (2011) The ecological significance of phenology in four different tree species: effects of light and temperature on bud burst. Int J Biometeorol 55:711–721.

Chapin FS III, Schulze ED, Mooney HA (1990) The ecology and economics of storage in plants. Annu Rev Ecol Syst 21:423–447.

Charrier G, Améglio T (2011) The timing of leaf fall affects cold acclimation by interactions with air temperature through water and carbohydrate contents. Environ Exp Bot 72:351–357.

Charrier G, Bonhomme M, Lacointe A, Améglio T (2011) Are budburst dates, dormancy and cold acclimation in walnut trees (*Juglans regia* L.) under mainly genotypic or environmental control? Int J Biometeorol 55:763–774.

Chen P, Li PH (1976) Effect of photoperiod, temperature and certain growth regulators on frost hardiness of *Solanum* species. Bot Gaz 137:105–109.

Choat B, Jansen S, Brodribb TJ et al. (2012) Global convergence in the vulnerability of forests to drought. Nature 491:752.

Cirelli D, Jagels R, Tyree MT (2008) Toward an improved model of maple sap exudation: the location and role of osmotic barriers in sugar maple, butternut and white birch. Tree Physiol 28:1145–1155.

Cochard H, Peiffer M, Le Gall K, Granier A (1997) Developmental control of xylem hydraulic resistances and vulnerability to embolism in *Fraxinus excelsior* L. Impacts on water relations. J Exp Bot 48:655–663.

Cochard H, Tyree MT (1990) Xylem dysfunction in *Quercus*: vessel sizes, tyloses, cavitation and seasonal changes in embolism. Tree Physiol 6:393–407.

Cochard H, Bodet C, Améglio T, Cruiziat P (2000) Cryo-scanning electron microscopy observations of vessel content during transpiration in walnut petioles. Facts or artifacts? Plant Physiol 124:1191–1202.

Cochard H, Lemoine D, Améglio T, Granier A (2001) Mechanisms of xylem recovery from winter embolism in *Fagus sylvatica* L. Tree Physiol 21:27–33.

Cruiziat P, Cochard H, Améglio T (2002) Hydraulic architecture of trees: main concepts and results. Ann For Sci 59:723–752.

Davis SD, Sperry JS, Hacke UG (1999) The relationship between xylem conduit diameter and cavitation caused by freezing. Am J Bot 86:1367–1372.

Ewers FW, Améglio T, Cochard H, Beaujard F, Martignac M, Vandame M, Bodet C, Cruiziat P (2001) Seasonal variation in xylem pressure of walnut trees: root and stem pressures. Tree Physiol 21:1123–1132.

Ewers FW, Lawson MC, Bowen TJ, Davis SD (2003) Freeze/thaw stress in *Ceanothus* of southern California chaparral. Oecologia 136:213–219.

Feild TS, Brodribb T (2001) Stem water transport and freeze-thaw xylem embolism in conifers and angiosperms in a Tasmanian treeline heath. Oecologia 127:314–320.

Gusta LV, Wisniewski M, Nesbitt NT, Gusta ML (2004) The effect of water, sugars, and proteins on the pattern of ice nucleation and propagation in acclimated and nonacclimated canola leaves. Plant Physiol 135:1642–1653.

Hacke U, Sauter JJ (1996) Xylem dysfunction during winter and recovery of hydraulic conductivity in diffuse-porous and ring-porous trees. Oecologia 105:435–439.

Hoch G, Körner C (2003) The carbon charging of pines at the climatic treeline: a global comparison. Oecologia 135:10–21.

Huner NPA, Öquist G, Sarhan F (1998) Energy balance and acclimation to light and cold. Trends Plant Sci 3:224–230.

Körner C (1998) A re-assessment of high elevation treeline positions and their explanation. Oecologia 115:445–459.

Langan SJ, Ewers FW, Davis SD (1997) Xylem dysfunction caused by water stress and freezing in two species of co-occurring chaparral shrubs. Plant Cell Environ 20:425–437.

Larcher W, Mair B (1968) Das Kälteresistenzverhalten von *Quercus pubescens*, *Ostrya carpinifolia* und *Fraxinus ornus* auf drei thermisch unterschiedlichen Standorten. Oecol Plant 3:255–270.

Lasheen AM, Chaplin CE (1971) Biochemical comparison of seasonal variations in three peach cultivars differing in cold hardiness. J Am Soc Hortic Sci 96:154–159.

Le Roux X, Walcroft AS, Daudet FA, Sinoquet H, Chaves MM, Rodrigues A, Osorio L (2001) Photosynthetic light acclimation in peach leaves: importance of changes in mass : area ratio, nitrogen concentration, and leaf nitrogen partitioning. Tree Physiol 21:377–386.

Leinonen I, Hänninen H (2002) Adaptation of the timing of bud burst of Norway spruce to temperate and boreal climates. Silva Fennica 36:695–701.

Levitt J (1980) Responses of plants to environmental stresses. Vol. 1. Chilling, freezing, and high temperature stress. Academic Press, New York, 497 pp.

Li C, Junttila O, Ernstsen A, Heino P, Palva ET (2003) Photoperiodic control of growth, cold acclimation and dormancy development in silver birch (*Betula pendula*) ecotypes. Physiol Plant 117:206–212.

Mayr S, Charra-Vaskou K (2007) Winter at the alpine timberline causes complex within-tree patterns of water potential and embolism in *Picea abies*. Physiol Plant 131:131–139.

Mayr S, Cochard H, Améglio T, Kikuta SB (2007) Embolism formation during freezing in the wood of *Picea abies*. Plant Physiol 143:60–67.

Medeiros JS, Pockman WT (2010) Carbon gain and hydraulic limits on water use differ between size classes of *Larrea tridentata*. J Arid Environ 74:1121–1129.

Meier U (2001) Stades phénologiques des mono- et dicotylédones cultivées. BBCH Monographie, Centre Fédéral de Recherche Biologiques pour l'Agriculture et les Forêts.

Milburn JA, Zimmermann MH (1986) Sapflow in the sugar maple in the leafless state. J Plant Physiol 124:331–344.

Morin X, Améglio T, Ahas R, Kurz-Besson C, Lanta V, Lebourgeois F, Miglietta F, Chuine I (2007) Variation in cold hardiness and carbohydrate concentration from dormancy induction to bud burst among provenances of three European oak species. Tree Physiol 27:817–825.

Morin X, Lechowicz MJ, Augspurger C, O'Keefe J, Viner D, Chuine I (2009) Leaf phenology in 22 North American tree species during the 21st century. Glob Chang Biol 15:961–975.

Nilsson JE, Walfridsson EA (1995) Phenological variation among plus-tree clones of *Pinus sylvestris* (L.) in northern Sweden. Silvae Genet 44:20–28.

Ögren E (1999) Fall frost resistance in willows used for biomass production. II. Predictive relationships with sugar concentration and dry matter content. Tree Physiol 19:755–760.

Pittermann J (2010) The evolution of water transport in plants: an integrated approach. Geobiology 8:112–139.

Pittermann J, Sperry JS (2003) Tracheid diameter is the key trait determining the extent of freezing-induced embolism in conifers. Tree Physiol 23:907–914.

Pittermann J, Sperry JS (2006) Analysis of freeze–thaw embolism in conifers. The interaction between cavitation pressure and tracheid size. Plant Physiol 140:374–382.

Pockman WT, Sperry JS (1997) Freezing-induced xylem cavitation and the northern limit of *Larrea tridentata*. Oecologia 109:19–27.

Poirier M, Lacointe A, Améglio T (2010) A semi-physiological model of cold hardening and dehardening in walnut stem. Tree Physiol 30:1555–1569.

Pratt RB, Ewers FW, Lawson MC, Jacobsen AL, Brediger MM, Davis SD (2005) Mechanisms for tolerating freeze–thaw stress of two evergreen chaparral species: *Rhus ovata* and *Malosma laurina* (Anacardiaceae). Am J Bot 92:1102–1113.

Pratt RB, Jacobsen AL, Mohla R, Ewers FW, Davis SD (2008) Linkage between water stress tolerance and life history type in seedlings of nine chaparral species (Rhamnaceae). J Ecol 96:1252–1265.

Pratt RB, North GB, Jacobsen AL, Ewers FW, Davis SD (2010) Xylem root and shoot hydraulics is linked to life history type in chaparral seedlings. Funct Ecol 24:70–81.

R Development Core Team (2005) R: a language and environment for statistical computing. R Foundation for Statistical Computing, Vienna, Austria. ISBN 3-900051-07-0, URL: http://www.R-project.org.

Rameau JC, Mansion D, Dumé G, Timbal J, Lecointe A, Dupont P, Keller R (1989) In: Flore forestière française. I Plaines et Collines, eds. Institut pour le développement forestier, Paris, 1785 pp.

Rameau JC, Mansion D, Dumé G, Timbal J, Lecointe A, Dupont P, Keller R (1993) In: Flore forestière française. II Montagnes, eds. Institut pour le développement forestier, Paris, 2421 pp.

Repo T, Lappi J (1989) Estimation of standard error of impedance-estimated frost resistance. Scand J For Res 4:67–74.

Rodrigo J (2000) Spring frosts in deciduous fruit trees—morphological damage and flower hardiness. Sci Hortic 85:155–173.

Sakai A (1966) Studies of frost hardiness in woody plants. II. Effect of temperature on hardening. Plant Physiol 41:353–359.

Sakai A, Larcher W (1987) Frost survival of plants. Responses and adaptation to freezing stress. Ecological studies 62. Springer, Berlin, 321 pp.

Sakr S, Alves G, Morillon RL, Maurel K, Decourteix M, Guilliot A, Fleurat-Lessard P, Julien JL, Chrispeels MJ (2003) Plasma membrane aquaporins are involved in winter embolism recovery in walnut tree. Plant Physiol 133:630–641.

Sauter JJ, Wisniewski M, Witt W (1996) Interrelationships between ultrastructure, sugar levels, and frost hardiness of ray parenchyma cells during frost acclimation and deacclimation in poplar (*Populus × canadensis* Moench Robusta) wood. J Plant Physiol 149:451–461.

Schreiber SG, Hamann A, Hacke UG, Thomas BR (2013) Sixteen years of winter stress: an assessment of cold hardiness, growth performance and survival of hybrid poplar clones at boreal planting site. Plant Cell Environ 36:419–428.

Shi P, Körner C, Hoch G (2008) A test of the growth-limitation theory for alpine tree line formation in evergreen and deciduous taxa of the eastern Himalayas. Funct Ecol 22:213–220.

Siminovitch D, Wilson CM, Briggs DR (1953) Studies on the chemistry of the living bark of the black locust in relation to its frost hardiness. V. Seasonal transformations and variations in the carbohydrates: starch–sucrose interconversions. Plant Physiol 28:383–400.

Sperry JS, Sullivan JEM (1992) Xylem embolism in response to freeze-thaw cycles and water stress in ring-porous, diffuse-porous and conifer species. Plant Physiol 100:605–613.

Sperry JS, Robson DG (2001) Xylem cavitation and freezing in conifers. In: Colombo S, Bigras F (eds) Conifer cold hardiness, Kluwer Academic Publishers, Dordrecht, pp 121–136.

Sperry JS, Holbrook NM, Zimmermann MH, Tyree MT (1987) Spring filling of xylem vessels in wild grapevine. Plant Physiol 83:414–417.

Sperry JS, Donnelly JR, Tyree MT (1988) Seasonal occurrence of xylem embolism in sugar maple (*Acer saccharum*). Am J Bot 75:1212–1218.

Stattin E, Verhoef N, Balk P, van Wordragen M, Lindstrom A (2012) Development of a molecular test to determine the vitality status of Norway spruce (*Picea abies*) seedlings during frozen storage. New For 43:665–678.

Strimbeck RG, Kjellsen TD, Schaberg PG, Murakami PF (2008) Dynamics of low-temperature acclimation in temperate and boreal conifer foliage in a mild winter climate. Tree Physiol 28:1365–1374.

Stuart SA, Choat B, Martin KC, Holbrook NM, Ball MC (2007) The role of freezing in setting the latitudinal limits of mangrove forests. New Phytol 173:576–583.

Sutinen ML, Palta JP, Reich PB (1992) Seasonal differences in freezing stress resistance of needles of *Pinus nigra* and *Pinus resinosa*: evaluation of the electrolyte leakage method. Tree Physiol 11:241–254.

Tanino K, Weiser CJ, Fuchigami LH, Chen THH (1990) Water-content during abscisic-acid induced freezing tolerance in bromegrass cells. Plant Physiol 93:460–464.

Thomas FM, Meyer G, Popp M (2004) Effects of defoliation on the frost hardiness and the concentrations of soluble sugars and cyclitols in the bark tissue of pedunculate oak (*Quercus robur* L.). Ann For Sci 61:455–463.

Tyree MT, Yang S (1992) Hydraulic conductivity recovery versus water pressure in xylem of *Acer saccharum*. Plant Physiol 100:669–676.

Tyree MT, Cochard H (1996) Summer and winter embolism in oak. Impact on water relations. Ann Sci For 53:173–180.

Vitasse Y, Porte AJ, Kremer A, Michalet R, Delzon S (2009) Responses of canopy duration to temperature changes in four temperate tree species: relative contributions of spring and autumn leaf phenology. Oecologia 161:187–198.

Yang S, Tyree MT (1992) A theoretical model of hydraulic conductivity recovery from embolism with comparison to experimental data on *Acer saccharum*. Plant Cell Environ 15:633–643.

Zhang MIN, Willison JHM (1987) An improved conductivity method for the measurement of frost hardiness. Can J Bot 65:710–715.

Zhu XB, Cox RM, Bourque CPA, Arp PA (2002) Thaw effects on cold-hardiness parameters in yellow birch. Can J Bot 80:390–398.

Zimmermann MH (1983) Xylem structure and the ascent of sap. Springer, Berlin, 143 pp.

Zwiazek JJ, Renault S, Croser C, Hansen J, Beck E (2001) Biochemical and biophysical changes in relation to cold hardiness. In: Colombo S, Bigras F (eds) Conifer cold hardiness. Kluwer Academic Publishers, Dordrecht, pp 165–186.